LBNL-40368
UC-405
Preprint

ERNEST ORLANDO LAWRENCE BERKELEY NATIONAL LABORATORY

A Numerical Study of the Kosterlitz-Thouless Transition in a Two Dimensional Coulomb or Vortex Gas

Raz Kupferman and Alexandre J. Chorin
Computing Sciences Directorate
Mathematics Department

May 1997
To be submitted for publication

REFERENCE COPY
Does Not
Circulate
Bldg. 50 Library - Ref.
Lawrence Berkeley National Laboratory
Copy 1
LBNL-40368

DISCLAIMER

This document was prepared as an account of work sponsored by the United States Government. While this document is believed to contain correct information, neither the United States Government nor any agency thereof, nor the Regents of the University of California, nor any of their employees, makes any warranty, express or implied, or assumes any legal responsibility for the accuracy, completeness, or usefulness of any information, apparatus, product, or process disclosed, or represents that its use would not infringe privately owned rights. Reference herein to any specific commercial product, process, or service by its trade name, trademark, manufacturer, or otherwise, does not necessarily constitute or imply its endorsement, recommendation, or favoring by the United States Government or any agency thereof, or the Regents of the University of California. The views and opinions of authors expressed herein do not necessarily state or reflect those of the United States Government or any agency thereof or the Regents of the University of California.

LBNL-40368

A NUMERICAL STUDY OF THE KOSTERLITZ-THOULESS TRANSITION IN A TWO DIMENSIONAL COULOMB OR VORTEX GAS*

Raz Kupferman and Alexandre J. Chorin
Mathematics Department
Lawrence Berkeley National Laboratory
University of California
Berkeley, CA 94720

May 1997

* This work was supported by the Applied Mathematical Sciences Subprogram of the Office of Energy Research, Department of Energy under contract DE-AC03-76SF00098.

A numerical study of the Kosterlitz-Thouless transition in a two-dimensional Coulomb or vortex gas

Raz Kupferman and Alexandre J. Chorin

Mathematics Department
Lawrence Berkeley National Laboratory
1 Cyclotron Road, 50A-2152
Berkeley, CA 94720

May 27, 1997

Abstract

Recent work has cast doubt on some of the usual assumptions in the analysis of the Kosterlitz-Thouless transition in a Coulomb or vortex gas; in particular, the well-known Kosterlitz-Thouless parameter flow appears to depend on some specific and somewhat implausible assumptions. In the present paper we extend this analysis and assess recent efforts to verify the properties of this transition numerically. We find that the verification depends critically on the availability and on the specific form of a finite-size scaling; we show that several alternative models cannot be properly considered with available numerical methods, and that the validity of the finite-size scaling is doubtful; with these caveats, we find that the numerical calculation of the phase transition line in the low-density regime agrees with the predictions of the usual KT theory with surprising accuracy. Several attendant paradoxes are also discussed.

1 Introduction

The Kosterlitz-Thouless transition is the transition between a conducting and an insulating phase in a sparse Coulomb system in the plane; it is also a basic paradigm in statistical physics, has been extended to the analysis of transitions in vortex and other two-dimensional systems, and constitutes a model for transitions in more dimensions. A basic theory of mean-field type for this system was given by Kosterlitz and Thouless (KT) several decades ago [1]; in particular, these authors sketched the famous renormalization group parameter flow that has remained the basic building block of subsequent work. Rigorous work on this transition is available, and modern approaches to the renormalization group have also appeared and provided higher order corrections to the basic theory [2, 3, 4]. For the sake of brevity, we shall use throughout a terminology appropriate for a Coulomb system.

Numerical work intended to check this theory has a long history [5, 6] and there is a substantial amount of recent work [7, 8, 9, 10, 11, 12, 13]. It was always clear that the verification of the properties of what is a very weak transition is difficult, but it is reasonable to expect that the properties of a two-dimensional system can nowadays be established with some certainty; recent work does indeed claim to have verified the basic properties of the Kosterlitz-Thouless parameter flow.

In a recent paper [14], Chorin and Hald showed that, within the framework of the simplest and oldest description of the transition, one can derive essentially different models with distinct properties; historically influential arguments that these models are equivalent contain fundamental errors. A further conclusion was that the correctness of the Kosterlitz-Thouless renormalization flow rests on a very specific assumption of one-sided polarization, which has long been known to be implausible in its literal form [15]. In further work, still unpublished, these authors have reached similar conclusions for more sophisticated derivations of the renormalization group equations. The conclusion that one-sided polarization was a key to the validity of the Kosterlitz-Thouless model has also been reached by Alastuey and Kornu by other means [16] and a further example that supports this conclusion will be given below. A conclusion from this work is that the validity of the basic theory is far from being firmly established on theoretical grounds. A further reason for doubting the standard theory is the recent discovery that well-known and long undoubted scaling properties of dense vortex systems are in fact in error [17].

In the present paper we reconsider recent numerical work on the KT transition, check it

and assess it. The key issue is the validity and significance of the finite-size scaling without which the calculations cannot be brought to a conclusion. As a check on our understanding of the numerical issues, we reconstructed much of the earlier work. The conclusion is that on the whole those aspects of the KT descriptions that are accessible to a numerical calculation with the available tools are verified with unexpected accuracy, indeed, with amazing accuracy; paradoxes and uncertainties still remain, and we shall discuss them. The emphasis here is on calculations in which the basic variables are the charges, but we believe that the conclusions illuminate what happens in other variables as well.

We consider the Coulomb gas in a periodic box, and its limiting behavior as the box size tends to infinity; we have no tools that would allow us to look at the KT problem in the whole plane, or to estimate the differences between the whole-plane problem and the limit of the periodic problem (a short discussion of the differences between these problems will be given). We focus on the behavior of the (possibly non-universal) phase transition line, the other properties of the transition being out of numerical reach. We provide a new example that shows the dependence of the phase transition line on the one-sided polarization assumption. With the help of some additional technical assumptions, we calculate the phase transition line and we find that it coincides, with surprising accuracy, with the predictions of the classical KT theory. The calculation exhibits some surprising and unexplained features. We believe that we provide the sharpest comparison so far between the original KT phase transition line and the numerical results.

The paper is organized as follows: We begin with a description of the Coulomb system, followed by a review of the relevant linear response theory and a summary of the conclusions of Chorin and Hald with a new example that illustrates them. We then explain the numerical approach and implement it with care. The conclusions and the remaining open questions are summarized in a final section.

2 The Coulomb gas in the plane

Consider a two-dimensional Coulomb gas with $2N$ particles that carry a unit charge $q = \pm 1$, in an $L \times L$ square box. Without loss of generality, one can assume that the gas is neutral [18], and thus to each positive charge corresponds a negative charge, with N being the number of pairs of opposite charges.

The Hamiltonian of the system is

$$H = \frac{1}{2}\int d\mathbf{x} \int d\mathbf{x}'\, \rho(\mathbf{x})G(\mathbf{x}-\mathbf{x}')\rho(\mathbf{x}'), \tag{1}$$

where $\rho(\mathbf{x})$ is the charge density, and $G(\mathbf{x})$ is the Green function of the Coulomb interaction which satisfies

$$\nabla^2 G(\mathbf{x}) = -2\pi\delta(\mathbf{x}), \tag{2}$$

subject to appropriate boundary conditions. For an infinite system $G(\mathbf{x}) = -\log|\mathbf{x}| + C$, where C is a constant. Simulations are however restricted to finite systems. It is usual and reasonable to work with periodic finite systems.

The interaction between point charges diverges logarithmically at short distance and it is necessary to introduce a cut-off length, σ, for the system to be stable. In a lattice model the cut-off is built-in if particles are prevented from occupying the same lattice site. In a continuum model a cut-off can be introduced by excluding configurations in which the separation between any two particles is less than a minimum length (a "hard core" model). A standard alternative is to regularize the interaction by smoothing the charge distribution $\phi(\mathbf{x}-\mathbf{x}_i)$ associated with each particle (a "soft core" model). We assume each particle has a Gaussian charge density profile [13], so that the charge density field is

$$\rho(\mathbf{x}) = \sum_{i=1}^{2N} q_i\phi(\mathbf{x}-\mathbf{x}_i) = \frac{1}{2\pi\sigma^2}\sum_{i=1}^{2N} q_i e^{-|\mathbf{x}-\mathbf{x}_i|^2/2\sigma^2}. \tag{3}$$

After substitution of (3) into (1) the Hamiltonian can be written as a double sum,

$$H_N(\{\mathbf{x}_i\}) = \frac{1}{2}\sum_{i=1}^{2N}\sum_{j=1}^{2N} q_i V(\mathbf{x}_i-\mathbf{x}_j)q_j, \tag{4}$$

where

$$V(\mathbf{x}_i-\mathbf{x}_j) = \int d\mathbf{x} \int dx'\, \phi(\mathbf{x}_i-\mathbf{x})G(\mathbf{x}-\mathbf{x}')\phi(\mathbf{x}_j-\mathbf{x}') \tag{5}$$

is the regularized interaction, which can be represented by the Fourier series

$$V(\mathbf{x}) = \frac{1}{2\pi}\sum_{\mathbf{k}\in\mathbb{Z}} \frac{1}{k^2}\exp\left(-\frac{4\pi\sigma^2}{L^2}k^2\right)\exp\left(\frac{2\pi}{L}i\mathbf{k}\cdot\mathbf{x}\right). \tag{6}$$

For $r \equiv |\mathbf{x}|$ small enough compared to the spatial period, L, $V(\mathbf{x})$ is spherically symmetric and approximated by

$$V(r) \simeq -\frac{1}{2}\left[\log\left(\frac{r^2}{4\sigma^2}\right) - \mathrm{Ei}\left(-\frac{r^2}{4\sigma^2}\right) + \gamma\right], \tag{7}$$

where $\mathrm{Ei}(\cdot)$ is the exponential-integral function [19], and γ is the Euler constant.

The critical properties of the Coulomb gas are characterized in particular by a sharp change in the response of the system to external fields. This response can be expressed by the dielectric "constant" ϵ, which is related to the two-point charge correlation function in the absence of external fields. The relation between the two is a standard result of linear response theory, which we review for the sake of clarity.

Consider an external electrostatic potential, $\Psi(\mathbf{x})$, which adds to the Hamiltonian a perturbation

$$\delta H = \int d\mathbf{x}\, \rho(\mathbf{x})\Psi(\mathbf{x}). \tag{8}$$

This external field induces a charge redistribution whose average in the linear response regime is

$$\langle \rho(\mathbf{x}) \rangle = -\beta \, \langle \rho(\mathbf{x})\, \delta H \rangle_0 \,, \tag{9}$$

where the notation $\langle \cdot \rangle_0$ refers to an average with respect to the unperturbed system. The induced charge distribution creates an electrostatic field, which together with $\Psi(\mathbf{x})$ forms an effective field,

$$\Psi^{\mathrm{eff}}(\mathbf{x}) = \Psi(\mathbf{x}) + \int d\mathbf{x}' \, \langle \rho(\mathbf{x}') \rangle \, G(\mathbf{x}-\mathbf{x}') \equiv \int d\mathbf{x}' \, \epsilon^{-1}(\mathbf{x}-\mathbf{x}')\Psi(\mathbf{x}'). \tag{10}$$

The last identity defines the inverse dielectric function $\epsilon^{-1}(\mathbf{x})$.

The inverse dielectric function is more easily expressed in Fourier space; let

$$\widehat{\epsilon^{-1}}(\mathbf{k}) = \frac{1}{L^2} \int d\mathbf{x}' \, \epsilon^{-1}(\mathbf{x}) \exp\left(-\frac{2\pi}{L}\mathbf{k}\cdot\mathbf{x}\right). \tag{11}$$

Equations (8)–(11) give

$$\widehat{\epsilon^{-1}}(\mathbf{k}) = 1 - \frac{\beta L^4}{2\pi k^2} \, \langle \hat{\rho}(\mathbf{k})\hat{\rho}(-\mathbf{k}) \rangle_0 \,, \tag{12}$$

with

$$\hat{\rho}(\mathbf{k})\hat{\rho}(-\mathbf{k}) = \frac{1}{L^4} \exp\left(-\frac{4\pi^2\sigma^2}{L^2}k^2\right) \left| \sum_{j=1}^{2N} q_j \exp\left(\frac{2\pi}{L} i\mathbf{k}\cdot\mathbf{x}_j\right) \right|^2 . \tag{13}$$

The components of the wave vector $\mathbf{k}$ in a finite periodic system with period L are multiples of $\frac{2\pi}{L}$. Note that a $\mathbf{k} = 0$ excitation corresponds to a uniform shift, which has no

physical effect on the system. Hence the smallest wave vector for which a dielectric response can be defined in a periodic system is $k = |\mathbf{k}| = \frac{2\pi}{L}$.

The inverse dielectric *constant*, ϵ^{-1}, is the $\mathbf{k} \to 0$ limit of $\widehat{\epsilon^{-1}}(\mathbf{k})$ in the thermodynamical limit. The two limits, $\mathbf{k} \to 0$ and $L \to \infty$, are not interchangeable, as the $\mathbf{k} \to 0$ limit is not defined for a finite system. In the simulations below we calculate the inverse dielectric function for the smallest nonzero wavevector. The inverse dielectric constant is the limit

$$\epsilon^{-1} = \lim_{L\to\infty} \widehat{\epsilon^{-1}}\left(\frac{2\pi}{L}\right). \tag{14}$$

It is often stated in the computational literature that it is necessary to extrapolate the inverse dielectric function calculated for finite wave numbers and fixed L to $\mathbf{k} = 0$. As the system size tends to infinity, both the $k = \frac{2\pi}{L}$ component of $\widehat{\epsilon^{-1}}(k)$ and the extrapolation to zero wave vector converge to the same limit and we see no reason to prefer the latter, which has no physical significance and contains an additional numerical error.

The statistical properties of a macroscopic system are determined by the probability measure associated with its microscopic states. We shall use both the canonical and the grand-canonical ensembles in the analysis of the system. In the canonical ensemble N, the number of pairs, is fixed, and the probability density function for the configuration $\{\mathbf{x}_i\}$ is the Boltzmann distribution,

$$p(\{\mathbf{x}_i\})\left(\prod_{j=1}^{2N} d\mathbf{x}_j\right) = \frac{1}{Z_c} e^{-\beta H_N(\{\mathbf{x}_i\})}\left(\prod_{j=1}^{2N} d\mathbf{x}_j\right), \tag{15}$$

where Z_c is the canonical partition function and $\beta \equiv \frac{1}{T}$ is the inverse temperature.

In the grand-canonical ensemble the number of pairs can vary, and a chemical potential or an energy per charge μ is introduced. It is convenient to start with a system in which the number of states is countable; let ζ be a spatial discretization size; the continuum limit will be recovered below. The probability density function for a state with N pairs and a configuration $\{\mathbf{x}_i\}$ is

$$p(N, \{\mathbf{x}_i\})\left(\prod_{j=1}^{2N} \frac{\Delta\mathbf{x}_j}{\zeta^2}\right) = \frac{1}{Z_{gc}} z^N e^{-\beta H_N(\{\mathbf{x}_i\})}\left(\prod_{j=1}^{2N} \frac{\Delta\mathbf{x}_j}{\zeta^2}\right), \tag{16}$$

where Z_{gc} is the grand-partition function, and $z = e^{2\beta\mu}$ is the fugacity.

The Coulomb gas model we have just defined involves the following parameters: the temperature T, the number of charge pairs N or alternatively the fugacity z, the system

size L, and the cut-off length σ. In the grand-canonical ensemble we also introduced a lattice size ζ. This system exhibits interesting scaling properties, which reduce the number of independent parameters and provide insight on the role of the cut-off length.

Consider equation (16): If the grid size ζ is small compared with the interaction cut-off length σ, the statistical properties of the system are asymptotically invariant under the grid refinement transformation,

$$\zeta \to \alpha\zeta \qquad z \to \alpha^4 z \qquad T \to T \qquad \sigma \to \sigma \qquad L \to L. \tag{17}$$

This suggests the definition of a rescaled fugacity, $\bar{z} \equiv \frac{z}{\zeta^4}$, which remains invariant under grid refinement. The continuum limit can then be taken by keeping $\bar{z}$ fixed while $\zeta \to 0$.

Another scaling relation follows from the fact that both the regularized interaction (6) and the inverse dielectric function (11) depend only on the length ratios, $\mathbf{x}_i/L$ and σ/L. Therefore the dielectric function remains invariant under the scaling transformation

$$\sigma \to \alpha\sigma \qquad L \to \alpha L \qquad \bar{z} \to \alpha^{-4}\bar{z} \qquad T \to T. \tag{18}$$

Two results follow from this invariance: (i) The cut-off length σ can always be set equal to one by an appropriate rescaling of the other parameters. (ii) The limit of point charges $\sigma \to 0$ with the other parameters fixed is equivalent to the limit of infinite fugacity or infinite particle density. The cut-off length determines the elementary length scale of the system, and certain quantities diverge as it tends to zero, as usual in the theory of phase transitions.

3 The KT renormalization group

Heuristically, the KT phase transition can be described as follows: At low temperatures all the particles form bound pairs of opposite charge and the medium is dielectric. At the critical temperature, T_c, charge unbinding occurs, and for $T > T_c$ there exist free charges which can conduct electric current and screen electric fields. The transition is accompanied by sharp changes in the dielectric constant and by the divergence of certain thermodynamic quantities [20].

In their original work [1] KT presented a model of the phase transition based on an iterated mean-field approach in the limit of low fugacity. In this model, at temperatures below the transition temperature, the medium is viewed as consisting of bound pairs of particles, or electric dipoles. In general, there is some ambiguity in the identification of the

pairs in a system in which only the coordinates of the individual charges are given; however, at low density this is not a serious problem.

Consider a dipole of size r; its contribution to the total energy can be divided into an intrinsic contribution $V(r)$ (the "bare" interaction), and the energy associated with its interaction with the rest of the system. In the mean-field approximation the interaction between charges that belong to different pairs is replaced by an ensemble average. The average energy of interaction between a dipole and the rest of the system is added to the bare interaction and defines an "effective", or renormalized, interaction energy. The total energy can then be written as a sum of the effective energies of the dipoles.

The effective energy $E(r)$ associated with a dipole of size r can be related to a scale-dependent dielectric function $\epsilon(r)$: Start with a dipole of size zero, and then increase its size adiabatically allowing the medium to equilibrate after each infinitesimal step. In the absence of neighboring charges, work is done against a restoring force $-\frac{\partial V}{\partial r}$. We introduce the dielectric function by writing the effective force as $-\epsilon^{-1}(r)\,\frac{\partial V}{\partial r}$. The effective energy of a dipole of size r is related to this function by

$$E(r) = -\int_0^r ds\,\epsilon^{-1}(s)\frac{\partial V}{\partial s}. \tag{19}$$

Note that both $V(r)$ and $\epsilon(r)$ are assumed to depend on the size of the dipole but not on its orientation. This approximation holds as long as the dipole is small compared to the size of the system. The lower limit of integration is taken as zero because the finite cut-off has already been taken into account in the definition of the regularized interaction, V.

At low fugacity, $\bar{z} \ll 1$, the density of dipoles of size between r and $r + dr$ is

$$dn(r) = 2\pi\bar{z}r\,dr\,\exp\left[\beta\int_0^r ds\,\epsilon^{-1}(s)\frac{\partial V}{\partial s}\right] + O\left(\bar{z}^2\right). \tag{20}$$

The polarizability of a dipole is $p(r) = \frac{1}{2}\beta r^2$ [1], and the electric susceptibility of the medium, χ, is the total polarizability per unit square,

$$\chi = \int_0^\infty dn(r)\,p(r) \simeq \pi\beta\bar{z}\int_0^\infty dr\,r^3\exp\left[\beta\int_0^r ds\,\epsilon^{-1}(s)\frac{\partial V}{\partial s}\right]. \tag{21}$$

where $n(r)$ is the number density of dipoles of size up to r. Finally the dielectric constant is related to the susceptibility by

$$\epsilon = 1 + 2\pi\chi \simeq 1 + 2\pi^2\beta\bar{z}\int_0^\infty dr\,r^3\exp\left[\beta\int_0^r ds\,\epsilon^{-1}(s)\frac{\partial V}{\partial s}\right]. \tag{22}$$

As pointed out in [14], equation (22) is not sufficient to determine the function $\epsilon(r)$; it is a single constraint on the infinite set of values of the function $\epsilon(r)$. One has to make additional assumptions to obtain a solvable model. The best known of the assumptions made by KT (for historical remarks, see e.g. [14]) was that equation (22) could be approximated by a scale dependent equation for the function $\epsilon(r)$

$$\epsilon(r) = 1 + 2\pi^2\beta\bar{z}\int_0^r dt\, t^3 \exp\left[\beta\int_0^t ds\, \epsilon^{-1}(s)\frac{\partial V}{\partial s}\right]. \tag{23}$$

The physical interpretation of this approximation is that the energy of a given dipole is reduced only by the polarization of dipoles that are smaller than itself. In particular, the energy of a dipole of size r is reduced by the polarization of a dipole of size $r - \delta r$ but not by the polarization of a pair of size $r + \delta r$, however small δr may be . At first sight, this is an implausible assumption.

It is customary to introduce a new function $K(r) \equiv \beta\epsilon^{-1}(r)$, in terms of which equation (23) becomes

$$K^{-1}(r) = \beta^{-1} + 2\pi^2\bar{z}\int_0^r dt\, t^3 \exp\left[\int_0^t ds\, K(s)\frac{\partial V}{\partial s}\right]. \tag{24}$$

The integro-differential equation (24) can be transformed into a system of first order differential equations. Define a logarithmic scale by $\ell = \log r$; equation (24) is then equivalent to the pair of ordinary differential equations

$$\begin{aligned} \frac{dK^{-1}}{d\ell} &= y(\ell) \\ \frac{dy}{d\ell} &= \left[4 - K(\ell)\left(1 - e^{-e^{2\ell}/4\sigma^2}\right)\right] y(\ell), \end{aligned} \tag{25}$$

with the initial conditions

$$\begin{aligned} &K^{-1}(\ell = -\infty) = T \\ &y(\ell) \sim 2\pi^2\bar{z}\, e^{4\ell}, \qquad \text{for } \ell \ll -1. \end{aligned} \tag{26}$$

The equivalence is in the sense of ordinary calculus: Integration of equations (25) yields values of the function $K(r)$ in (24). However, equations (25) can also be given an interesting additional interpretation: One can view $y(\ell)$ and $\beta/K^{-1}(\ell)$ as the effective fugacity and dielectric constant at scale ℓ, and thus equations (25) describe the flow of the parameters as functions of scale; they can thus be viewed as renormalization group (RG) equations.

On the basis of this model one can also calculate $n(r)$, the density of dipoles of size smaller than r, which satisfies the differential equation

$$\frac{dn}{d\ell} = \frac{e^{-2\ell}}{\pi} y(\ell), \tag{27}$$

with the initial condition $n(-\infty) = 0$.

The RG equations (25) differ slightly from their standard form because we accounted explicitly for the effect of a regularized interaction, $V(r)$. This correction to the equations becomes small as $\ell \gg 1$. One normally assumes that the universal properties of the system are determined by the properties of the fixed point of the renormalization flow [21], while the precise location of the phase transition line, which can be read from these equations as well, may well depend on the contingencies of the cut-off and of the specific assumptions used to derive the RG equations from the more general statement of the linear response assumption.

The macroscopic inverse dielectric constant is the asymptotic value $\epsilon^{-1} = TK(\infty)$. The two parameters T and $\bar{z}$ determine the initial conditions (26) and thus determine ϵ^{-1}. For each value of $\bar{z}$ there exists a critical temperature $T_c(\bar{z})$; it is widely believed that at T_c the dielectric constant ϵ^{-1} jumps discontinuously from a finite value [20].

The critical behavior of the system can be read from equations (25) as follows: For $\ell \gg 1$ the derivative $\frac{dy}{d\ell}$ simplifies into $[4 - K(\ell)]\, y(\ell)$, and the trajectories $(K(\ell), y(\ell))$ are given by a family of curves [14]

$$y = \log \frac{K}{4} + \frac{4}{K} - 1 + c(T, \bar{z}), \tag{28}$$

where $c(T, \bar{z})$ is a constant that characterizes the curve and is determined by the initial conditions. The resulting family of functions $y = y(K)$ has a vertical asymptote at $K = 0$, is decreasing for $0 < K < 4$, has a minimum $y_{min} = c(T, \bar{z})$ at $K = 4$, and increases for $K > 4$. Points at which these curves intersect the K-axis are fixed points, hence y does not change sign along a trajectory. As $K(-\infty) > 0$ and $y(-\infty) > 0$, $y(\ell)$ is always positive and $K(\ell)$ is monotonically decreasing. The trajectory that passes through the fixed point $(K = 4, y = 0)$ is the critical trajectory which separates the parameter values for which $K_\infty \equiv K(\infty) = 0$ (the conducting phase) from those for which K_∞ is finite (the dielectric phase); see Figure 1. Note that this description of the phase transition contains a strong heuristic element; in [14] it is shown that the RG trajectories are not well-defined in the conducting phase. From equation (28) it follows that this fixed point is reached for $c = 0$, i.e., the condition $c(T_c, \bar{z}) = 0$ defines implicitly the critical curve $T_c(\bar{z})$. This observation is

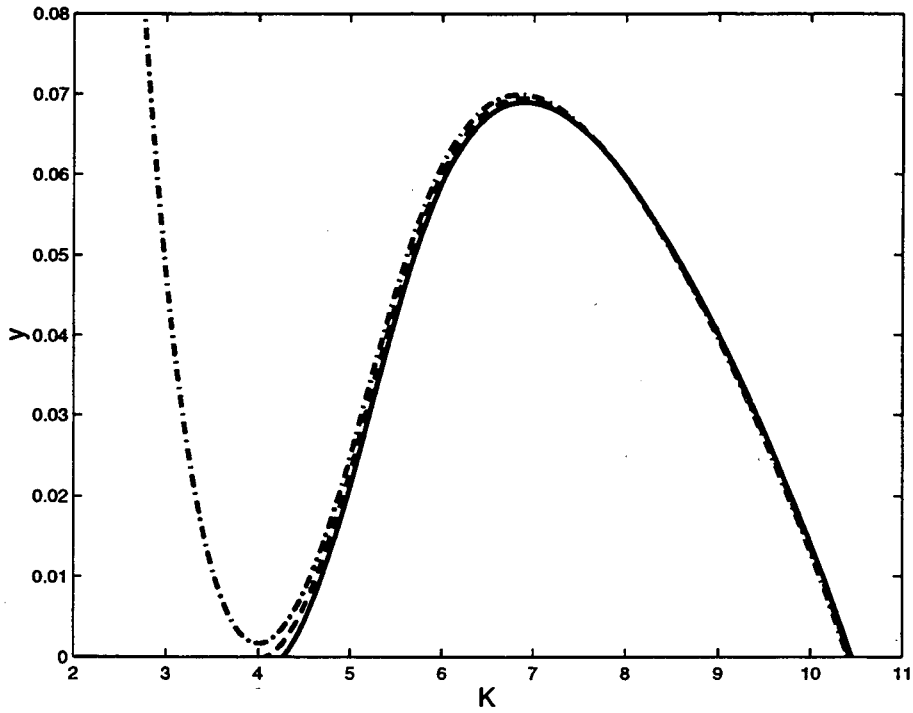

Figure 1: The K-y projection of the renormalization flow (25) for $\bar{z} = 0.006$, $T = 0.0957$ (solid line), $T = 0.0959$ (dashed line), and $T = 0.0961$ (dash-dot line).The initial condition is given by equations (26) with $\ell = -4.0$. The critical curve is the one that approaches the fixed point $(4, 0)$.

often interpreted as meaning that K_∞ jumps at the transition point from $K_\infty = \epsilon^{-1}/T = 4$ to 0, a conclusion known as the universal jump condition (but it should be pointed out that though the conclusion may well be true, it is shown in [14] that this derivation makes no mathematical sense).

The phase transition line determined from equations (25) is shown in Figure 2 where we plot trajectories $(K(\ell), y(\ell))$ calculated by a numerical integration of equations (25).

Equations (25) can be derived by more sophisticated means, together with higher order (in y) approximations; the most attractive alternative proceeds through the identification of the system with a Sine-Gordon field theory (see e.g [18]). However, for our present purposes the derivation above is sufficient. Our goal is to examine whether the phase transition can be described by equations (25) with their initial data; the identification of flaws in various derivations is outside the scope of the present paper.

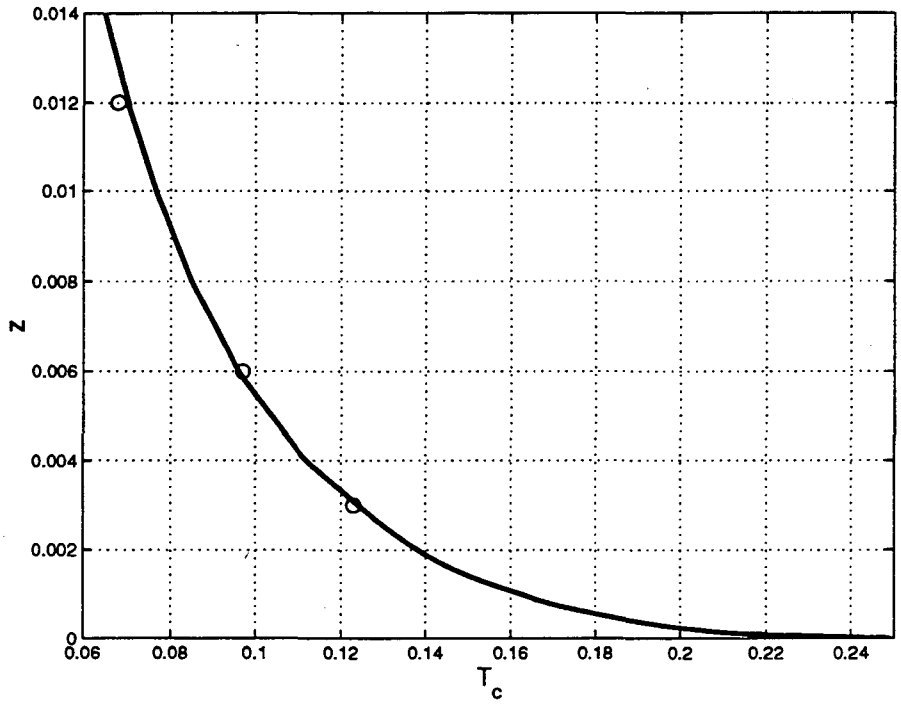

Figure 2: The phase transition line, $T_c(\bar{z})$, calculated from the renormalization group equations (25).

3.1 Alternative models

The KT model leading to equation (24) involves an additional assumption, needed to obtain a solvable model: The interactions between dipoles are assumed to be one-sided; dipole energies are affected only by the polarization of smaller dipoles. As was demonstrated in [14], the KT assumption is not the only one that can be made, and we have argued that it is implausible. Several other assumptions can be found in the literature. The general belief is that these other assumptions also lead to the KT parameter flow (equation (25)). In [14], Chorin and Hald showed that this general belief is false, and indeed that most of the derivations of the KT equations within the context of linear response theory are in error. Other *a priori* reasonable assumptions lead to phase transition lines different from the KT line in Fig 2, and to theories that are different both qualitatively and quantitatively.

Note that the models offered in [14] that are drastically different from the KT model are non-local, in the sense that the energy of a pair of any size is affected by the polarization of pairs of all sizes, large as well as small, but of course with weights that differ according to the relative size. In a finite calculation, there is no way to check the correspondence between

these different models and numerical results because all dipole pairs beyond the size of the computational domain are suppressed.

We now exhibit a simple model that demonstrates the sensitivity of the KT phase transition line to the specific assumption of one-sided polarization. Suppose that instead of having the dipoles of size up to r and no others affect the energy of a pair of size r, we allow also the pairs up to size αr to enter into the calculation of $K^{-1}(r)$, where α is a parameter. (This is a purely mathematical example, and no claim is made that it corresponds directly to some real physics; it is nonetheless not less plausible than the KT assumption.) The resulting integro-differential equation for $K(r)$ is

$$K^{-1}(r) = \beta^{-1} + 2\pi^2 \bar{z} \int_0^{\alpha r} dt\, t^3 \exp\left[\int_0^t ds\, K(s) \frac{\partial V}{\partial s}\right]. \tag{29}$$

This equation is also equivalent to a pair of (this time, non-local) ordinary differential equations,

$$\begin{aligned} \frac{dK^{-1}}{d\ell} &= y(\ell) \\ \frac{dy}{d\ell} &= y(\ell)\left[4 - y(\ell + \log\alpha)\left(1 - e^{-\alpha^2 e^{2\ell}/4\sigma^2}\right)\right]. \end{aligned} \tag{30}$$

The initial conditions are

$$\begin{aligned} K(-\infty) &= T \\ y(\ell) &\sim 2\pi^2 \bar{z} \alpha^4 e^{4\ell} \qquad \ell \ll -1. \end{aligned} \tag{31}$$

The solution of equations (30) depends on the value of α. However large ℓ may be, the solution of (30) never "forgets" its initial conditions, and some properties of the phase transition change. In particular, the location of the phase transition line changes with α. (See Figure 3). Thus a simple generalization of the sharp one-sidedness assumption of the KT model has a substantial effect on the phase transition line.

Note that as $\ell \to \infty$, the new RG equations (30) converge to the KT equations (25); indeed, for ℓ large enough, the non-local additive argument in K becomes negligible. By contrasting this remark with the theory in [14], we reach the following conjecture: All models of the phase transition in which the polarization of only a finite range of dipole sizes can affect the energy of a dipole of a given size give rise to RG equations with the same asymptotic properties near the critical point. However, this still allows the non-universal properties of the transition, for example the location of the phase transition line, to depend on the specific properties of the model; in the present case, the phase transition line is a sensitive function of α.

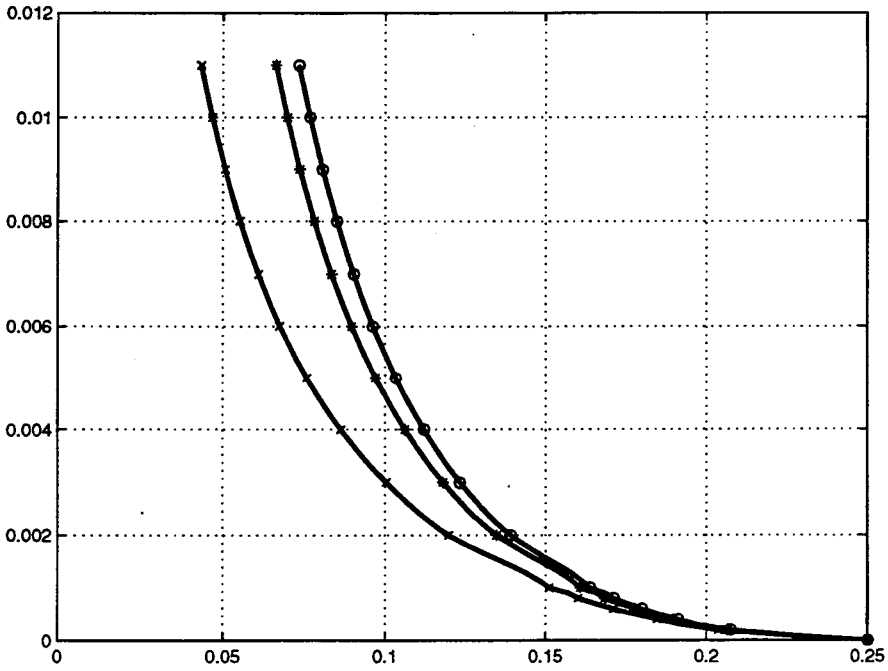

Figure 3: Phase transition lines, $T_c(\bar{z})$, calculated by solving the integro-differential equation (29) for three values of α: 1.0 (circles), 1.2 (stars), and 2.0 (crosses).

4 The numerical algorithm

We now turn to the numerical investigation of the KT transition. First the infinite plane must be approximated by a square, and it is generally believed that the boundary conditions that typically yield the highest accuracy (i.e., represent most faithfully what happens in the whole plain) are periodic boundary conditions. A major uncertainty is introduced in this way: It is far from obvious, and probably false in general, that the statistics of a Coulomb system in a finite domain, with any boundary conditions, converge to the statistics of a Coulomb system in the plane. Indeed, it is quite easy to see that the Coulomb interaction in the plane decays so slowly with distance that the effect of those charges that are outside a circle of radius R on the charges at the center of that circle does not tend to zero as R increases. By the same argument, models in which pairs of all sizes interact, such as the ones considered in [14], cannot be studied numerically on a finite domain. A whole class of interesting phenomena is therefore excluded at the outset. We are studying a problem that differs from the true problem, and are excluding models that differ from the bounded-interaction model and that would make sense only for the true problem. This limitation should not be forgotten.

The statistical properties of our Coulomb gas in a periodic domain can be calculated by Monte-Carlo methods, where averages are calculated over a Markov chain of states generated numerically. The standard way of doing so is the Metropolis algorithm, in which the Markov chain process is specified by transition probabilities $w_{i\to j}$ between states characterized by $(N_i, \{\mathbf{x}_i\})$ and $(N_j, \{\mathbf{x}_j\})$. For the statistical weight of the i'th state, p_i, to approach the desired equilibrium value, $p(N_i, \{\mathbf{x}_i\})$, as the size of the sample tends to infinity, it is sufficient (though not necessary) to impose the detailed balance condition

$$p(N_i, \{\mathbf{x}_i\})\, w_{i\to j} = p(N_j, \{\mathbf{x}_j\})\, w_{j\to i} \qquad \forall i, j. \tag{32}$$

This condition does not define the transition probabilities uniquely.

Previous numerical work has been based on the grand-canonical ensemble. The two ensembles lead to identical statistical properties in the thermodynamical limit, where number fluctuations are negligible. In the present problem however the simulations can only be performed with small systems in which these fluctuations are not necessarily small. It will therefore be of interest to compare the numerical results obtained with the two ensembles.

In the case of the canonical ensemble we proceed as follows: At each step one particle is

selected from the set of particles present, with each particle having an equal chance to be chosen. An attempt is then made to move it to a new location within a radius d from its current location; the new location is selected with uniform probability within the circle of radius d, and periodicity is enforced. This defines a trial move from a state $(N, \{\mathbf{x}_i\})$ to a state $(N, \{\mathbf{x}_j\})$, which is then accepted with probability $\min(1, \exp\{-\beta[H_N(\{\mathbf{x}_j\}) - H_N(\{\mathbf{x}_i\})]\})$.

This algorithm assigns non-zero probabilities only to transitions between states that differ in the location of one particle by a distance less than d. The attempt frequency between two states, i and j that are accessible to each other, i.e., the probability density of the event that there will an attempt to move the system from one of them to the other, is constant and equal to $\Omega_{i\to j} = \Omega_{j\to i} = \frac{1}{\pi d^2}$. The transition probability, $w_{i\to j}$, is the product of the attempt frequency, $\Omega_{i\to j}$, and of the acceptance probability, $a_{i\to j}$, that once the attempt is made, it will be accepted. This product satisfies the detailed balance condition,

$$\frac{w_{i\to j}}{w_{j\to i}} = \frac{a_{i\to j}}{a_{j\to i}} = e^{-\beta[H_N(\{\mathbf{x}_j\})-H_N(\{\mathbf{x}_i\})]}. \tag{33}$$

The Markov chain for the grand-canonical ensemble has to include transitions between states with differing numbers of particles. We construct a process in which each step can allow pair creation, particle displacement, or pair elimination. The type of trial move is selected at random, with probabilities $p_\uparrow$, p_0, and $p_\downarrow$, respectively, with $p_\uparrow = p_\downarrow$.

The relocation of particles is performed in exactly the same way as in the case of the canonical ensemble. Pair addition is implemented by randomly selecting two sites for the new particles to be added; the new sites are selected with uniform probability throughout the system. Again we need to briefly consider a lattice model with grid size ζ. Let $(N, \{\mathbf{x}_i\})$ and $(N+1, \{\mathbf{x}_j\})$ denote the state of the system before and after the addition of a pair. The attempt frequency for such a move is $\Omega_{i\to j} = p_\uparrow / \left(\frac{L}{\zeta}\right)^4$. The backward transition of pair elimination is performed by randomly selecting a positive and a negative charge to be removed. The attempt frequency in this case is $\Omega_{j\to i} = p_\downarrow/(N+1)^2$. For detailed balance to be satisfied, the acceptance probabilities, $a_{i\to j}$ and $a_{j\to i}$, must guarantee that

$$\frac{w_{i\to j}}{w_{j\to i}} = \frac{\Omega_{i\to j}\, a_{i\to j}}{\Omega_{j\to i}\, a_{j\to i}} = z\, \exp\{-\beta[H_{N+1}(\{\mathbf{x}_j\}) - H_N(\{\mathbf{x}_i\})]\}. \tag{34}$$

Therefore the ratio of acceptance probabilities is

$$\frac{a_{i\to j}}{a_{j\to i}} = \frac{L^4}{(N+1)^2}\frac{z}{\zeta^4} e^{-\beta[H_{N+1}(\{\mathbf{x}_j\})-H_N(\{\mathbf{x}_i\})]} \equiv R. \tag{35}$$

This relation is satisfied if we take, for example, $a_{i\to j} = \min(1, R)$ and $a_{j\to i} = \min(1, R^{-1})$. We can now reintroduce the rescaled fugacity, $\bar{z} = z/\zeta^4$, and let the lattice size go to zero.

The two algorithms defined above still include free parameters, such as d, $p_\uparrow$, and p_0, which can be dynamically adapted such to optimize the convergence rate of the Metropolis sampling. It is widely thought that an optimal convergence rate is obtained when the acceptance ratio of a single Metropolis step is $\frac{1}{2}$; indeed, if the acceptance ratio is too small the system will change very slowly, and if it is too large, it must be that the proposed moves are too small and the evolution will be slow as well.

4.1 Finite size scaling

A standard problem in Monte-Carlo simulations is the extrapolation of the numerical results to the thermodynamical limit. As explained above, the most we can obtain in a simulation is an evaluation of the inverse dielectric function for the smallest non-zero wave number, which depends in general on both the temperature T, and the size of the system L. The phase transition point, T_c, for a given chemical potential or density, can be located by the requirement that at T_c the dielectric *constant* (14) drops discontinuously from a finite value to zero. In doing so, we explicitly assume the correctness of the universal jump condition [20] for which an independent check would have been desirable. This discontinuity refers to the thermodynamical limit, hence we have to extrapolate the numerical results to this limit. The extrapolation of $\widehat{\epsilon^{-1}}\left(\frac{2\pi}{L}\right)$ to the thermodynamical limit requires the knowledge of the form of the dependence of ϵ on L. One can derive this dependence from the RG equations, but one has to be very careful not to base conclusions regarding the validity of the KT theory on a numerical process into which this theory is built in.

When $c(T, \bar{z}) = 0$ (i.e., at the critical temperature) and $\ell \gg 1$, the $(K(\ell), y(\ell))$ trajectory is given by the function

$$y(\ell) = \log \frac{K(\ell)}{4} + \frac{4}{K(\ell)} - 1 \tag{36}$$

[14]; substitution into equation (25) yields a closed equation for $K(\ell)$,

$$\frac{dK}{d\ell} = -K^2 \log \frac{K(\ell)}{4} + K(K-4). \tag{37}$$

Linearizing about the fixed point, $K(\ell) = 4 + \kappa(\ell)$, we find

$$\frac{d\kappa}{d\ell} = -\frac{1}{2}\kappa^2, \tag{38}$$

which is easily integrated. Hence

$$K(\ell) \sim 4\left[1 + \frac{1}{2(\ell + \ell_0)}\right] \qquad \ell \gg 1, \tag{39}$$

or, reverting to the original scale,

$$\epsilon^{-1}(r) = 4T\left[1 + \frac{1}{2\log(r/L_0)}\right] \qquad r \gg 1, \tag{40}$$

where ℓ_0 and L_0 are integration constants and $\ell_0 = -\log L_0$. Equation (40) is widely viewed as a plausible guess for the scale dependent dielectric function of the KT transition.

Note here a significant ambiguity: The parameter r refers to the size of a dipole; in the KT theory one assumes that the energy of a dipole depends on the polarization of smaller dipoles but not on the polarization of larger dipoles. If one identifies $\beta K - 1$ evaluated at L with the factor by which the energy of a pair of size L is decreased, one is making a non-trivial additional assumption according to which dipoles smaller than L outside the square of side L do not contribute to the dielectric response, and one also simplifies the complexities that arise when one has pairs smaller than L lie partly inside and partly outside the periodic box of side L. In other words, we are identifying, with no clear quantitative rationale, two quantities that are in principle different: (i) The reduction in the energy of a single dipole pair by an external field and (ii) the effective field resulting from the ensemble average over the charge distribution induced by the external field. What we calculate numerically is the response of our system to a spatially sinusoidal field with wave number $k = \frac{2\pi}{L}$. It is most unlikely that $\epsilon^{-1}(L)$, as defined by the KT model, and $\widehat{\epsilon^{-1}}\left(\frac{2\pi}{L}\right)$, as defined by equation (12), are the same quantity. The derivation of the form of the finite-size scaling cannot be taken literally. Note in addition that in a periodic system of size L the maximum separation between two points is $L/2$.

In a similar way, one finds $y(r)$ and $n(r)$,

$$y(r) \sim \frac{1}{8(\log r/L_0)^2} \tag{41}$$

$$n(r) \sim n_\infty - \frac{1}{8\pi}\left[\frac{1}{r^2 \log r/L_0} + \frac{2}{L_0^2}\mathrm{Ei}\left(-2\log\frac{r}{L_0}\right)\right]. \tag{42}$$

In addition, the relevance of the finite size scaling formula to the extrapolation of data obtained for finite (and small) systems should depend on the scale at which the behavior of $K(\ell)$ is well approximated by equation (39). From equation (39) it follows that

$$\frac{2}{K(\ell) - 4} \sim \ell + \ell_0 \tag{43}$$

for $\ell \gg 1$. In Figure 4a we plot $\frac{2}{K(\ell)-4}$ as function of ℓ for $\bar{z} = 0.003$, and eight different values of temperature. The thick solid line correspond to the critical temperature $T_c = 0.1229532$, and coincides with the line $\ell + 0.951$; thus $\ell_0 = 0.951$ or $L_0 = e^{-\ell_0} = 0.386$. The other lines correspond from top to bottom to the values of temperatures indicated in the legend of the figure. The further T is from T_c, the earlier does the curve deviate from the straight line. A deviation from the critical temperature at the seventh significant digit causes the curves to separate at the logarithmic scale of $\ell \sim 80$.

For the sake of comparison with the numerical simulations one needs to consider much smaller scales. In Figure 4b we present the same curves for $0 < \ell < 10$. The thick solid line is again the asymptotic behavior of the critical curve. None of these curves coincide with the asymptote in this range. For T very close to T_c there exists an intermediate range of scales where the behavior of the curves is linear; the slope of the curve is however not one as predicted by the finite size scaling formula. For $T = 0.1228$, which deviates from the critical temperature by a tenth of a percent, there is no range for which $\frac{2}{K(\ell)-4}$ is linear. The very high sensitivity of the renormalization flow to the temperature, and the fact that it agrees with the asymptotic behavior only at vary large scales, shed doubt on the extrapolation procedure based on the finite size scaling formulas.

An alternative to this finite size scaling, based on an analog of Callen-Symanzik form of the renormalization group, has been proposed for the spin version of the KT transition [8], and turned out to be inapplicable in our calculations, as we shall discuss further below.

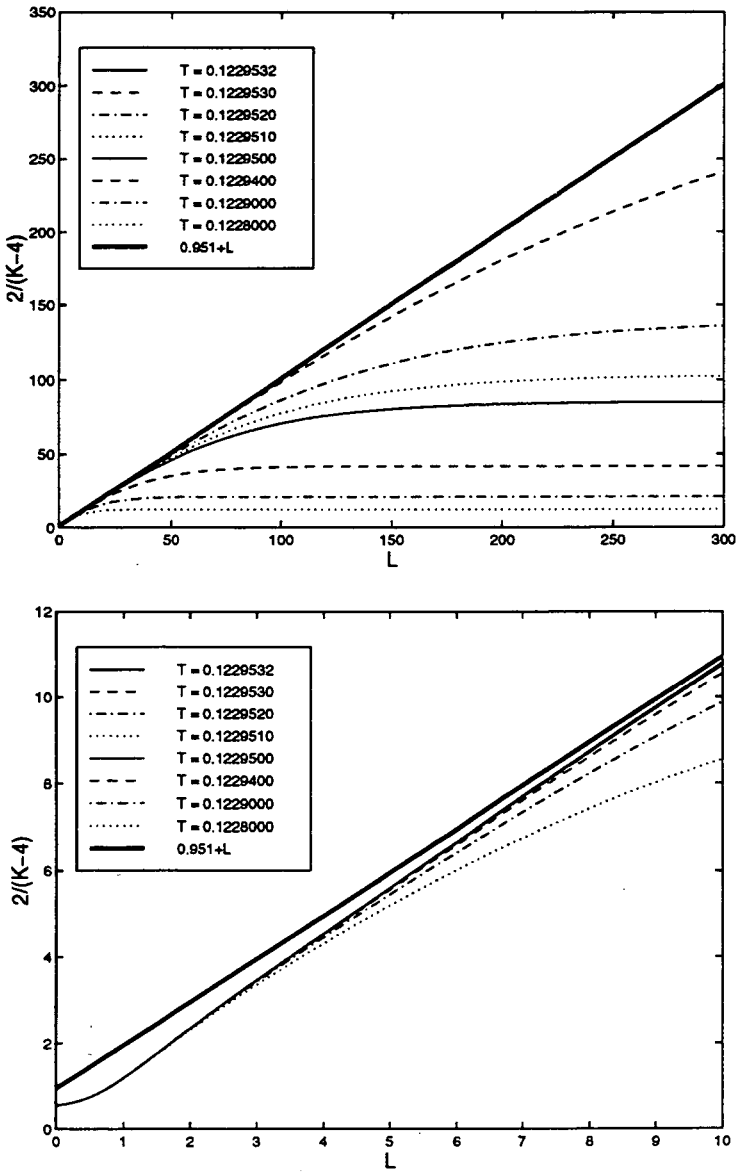

Figure 4: Evaluation of the asymptotic parameter ℓ_0 for $\bar{z} = 0.003$. The graphs show $\frac{2}{K(\ell)-4}$ versus the renormalization flow parameter ℓ. The thick solid line represents the asymptotic linear dependence at the critical point, $\frac{2}{K(\ell)-4} = \ell + \ell_0$ with $\ell_0 = 0.951$. The eight curves are for different values of the temperature (see legend). Figure (b) is a magnification of Figure (a) at small values of ℓ.

5 Comparisons with some earlier work

The early numerical work on the KT transition was related to the XY spin model [6]. These simulations attempted to validate the KT theory, but gave inconclusive results due to poor statistics. In order to have sufficient statistics one needs to have a large number of vortices. The vortex-pair density near the phase transition in the XY model is less than 10^{-2}, creating a need for very large systems.

Saito and Müller-Krumbhaar [5] were the first to study the XY model by explicitly considering vortex statistics, i.e., by studying a Coulomb gas. They used a lattice model with a chemical potential $\mu = -0.808$ which corresponds to half the energy of vortex-pair creation in the XY model. They were able to locate the transition from dielectric to metallic behavior within 20% accuracy.

Lee and Teitel [22] considered a lattice Coulomb gas with a variable chemical potential, defined by the Hamiltonian,

$$H = \frac{1}{2}\sum_i \sum_j q_i V(\mathbf{x}_i - \mathbf{x}_j) q_j - \mu \sum_i q_i^2 + \sum_i (q_i^4 - q_i^2), \tag{44}$$

where the summations run over all lattice points, q_i assumes all signed integers, and the last terms help to suppress charges with $|q_i| > 1$. They focused mainly on the first order transition to a solid-like checkerboard lattice, obtained for large negative values of the chemical potential. To locate the KT transition they calculated $\widehat{\epsilon^{-1}}\left(\frac{2\pi}{L}\right)$, and identified the transition point as the intersection of the curves of $\widehat{\epsilon^{-1}}\left(\frac{2\pi}{L}\right)$ as function of T for different sizes of system. This intersection point lies close to the line representing the universal jump condition, but does not coincide with it. In fact, it is not clear from the data that one should expect all the curves to intersect at one point for increasing system size.

The use of the finite size scaling relation to locate the KT transition was introduced by Weber and Minnhagen [7]. The derivation of the scaling relation from the KT renormalization group equations was, to our knowledge, first presented in [23]. For the XY model these authors were able to locate the transition point based on the best fit within a few tenth of percent. This approach was then adopted by numerous other authors [24, 12, 13].

As stated above, there is a difficulty in validating a theory with a calculation that explicitly uses the theory to be validated. We have been unable to avoid this vicious circle completely while using periodic boundary conditions. An interesting alternative is to use "self-consistent" boundary conditions [25], where the interaction of the environment with the

subsystem under consideration is approximated by an appropriate mean-field term added to the Hamiltonian. The idea is to pick an appropriate effective interaction such that (i) the modified Hamiltonian reduces to the original one in the thermodynamical limit, and (ii) there is only a weak dependence of the observable of interest on the size of the system. These two properties, if satisfied, may produce values of the observables for a finite domain that do not deviate much from their thermodynamical limits. Thus, the use of self-consistent boundary conditions may be a powerful alternative to the finite-size scaling discussed above, and is closely related to the Callen-Symanzik form of the RG [21].

Such an approach has been successfully applied to spin systems [26], where interactions are local, and therefore the environment interacts only with perimeter spins; this interaction can be modified by the introduction of a coupling constant that may have to satisfy some self-consistency conditions.

In the context of the KT transition, self-consistent boundary conditions were considered by Olsson [8, 9, 10, 11] in a spin formulation; the claim is that the results are promising, but not enough detail is given in the papers cited to compare in detail with the KT theory. The condition for the approach to work is that there exists a value of the coupling constant for which the derivative of the quantities of interest (for example, the dielectric constant) with respect to the size L of the computational domain vanishes; this value of the coupling constant presumably leads to the best values of the dielectric constant; the same holds for other quantities of interest, possibly at other values of the coupling constant. We have attempted to apply this method in the present problem, and found that with the obvious analog of the coupling used by Olsson the derivative of the dielectric constant with respect to the system size was a monotonically increasing function of the system size, i.e., the best value of the coupling constant was zero and the derivative was not zero at that point; thus the method, as we applied it, did not work. We expect to return to this problem in a future publication.

6 Numerical results

We now present the numerical results. The regularized interaction function was calculated from the Fourier series (6), and stored in a matrix for optimization purposes. The cut-off scale in all the simulations was chosen to be $\sigma = 1$. The number of Metropolis steps in each run was $5 \cdot 10^5 L^2$. The first 10% of the steps was excluded from the statistics in order to allow the system to equilibrate first.

We start with the canonical ensemble. To estimate the accuracy of the procedure we plot in Figure 5 the running average of $\widehat{\epsilon^{-1}}\left(\frac{2\pi}{L}\right)$ as function of the size of the sample. The three curves were calculated with the same values of parameters except for a different initialization seed for the random number generator. The convergence rate is expected to scale as the $(-\frac{1}{2})$ power of the size of the sample. From Figure 5 the error in the dielectric function can be estimated as fractions of a percent.

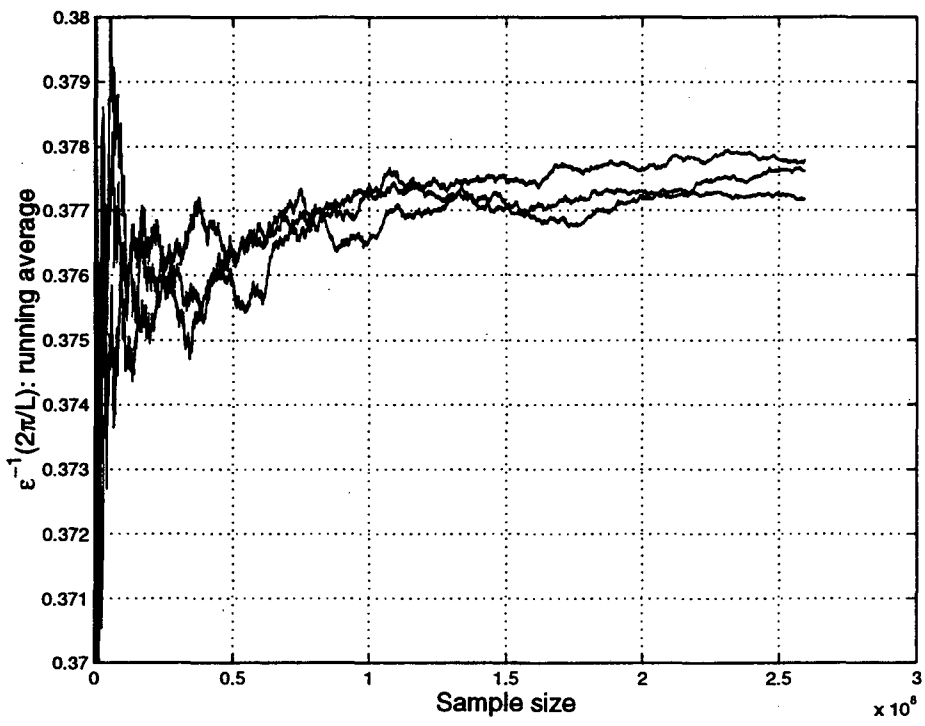

Figure 5: The running average of the inverse dielectric function for the smallest nonzero wavevector as function of the size of the sample for the canonical ensemble with $T = 0.08$, $N = 16$, and $L = 24$. The three curves were calculated with three different seeds to initialize the random number generator.

In Figure 6 we plot $\widehat{\epsilon^{-1}}\left(\frac{2\pi}{L}\right)$ as function of temperature for a dipole density of $n = 0.0277$.

The five curves correspond to five different system sizes. The dashed line is a graph of the universal jump condition, $4\epsilon^{-1}T = 1$. The dielectric function is, as expected, a decreasing function of temperature. This plot however is by itself insufficient to indicate the occurrence of a phase transition, and certainly does not allow to locate the phase transition point. Even if one relies on the theoretical prediction that the graph of $\epsilon^{-1}(T)$ intersects the universal jump curve at the critical point, it is not clear where this intersection occurs as $L \to \infty$.

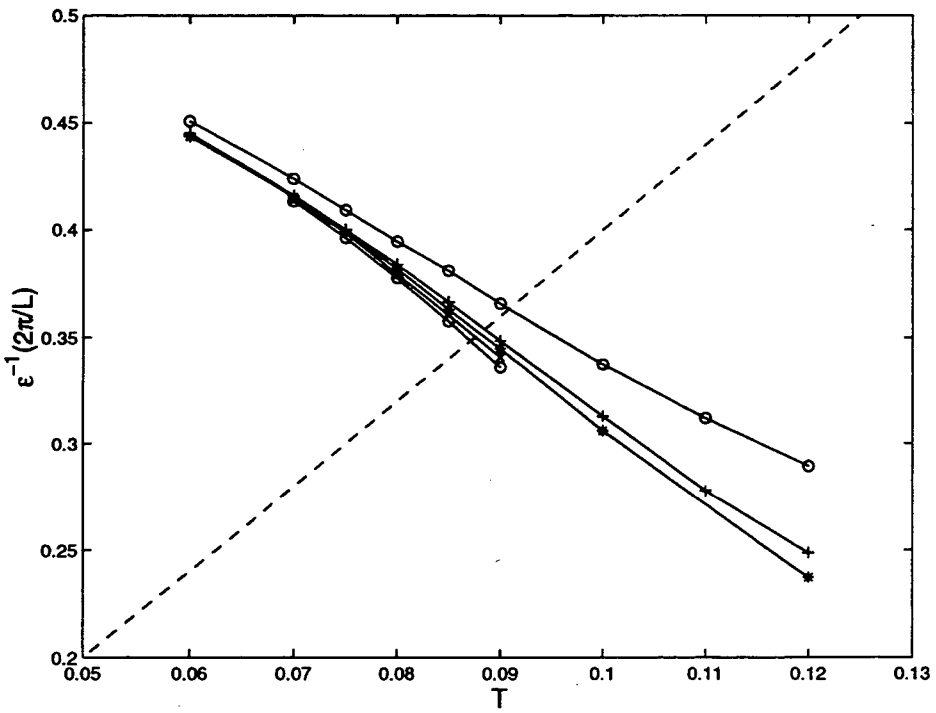

Figure 6: Canonical ensemble: the "bare" (uncorrected by finite-size scaling) inverse dielectric function for the smallest nonzero wavevector as function of temperature. The dipole density is $n = 1/36$. The five curves correspond from top to bottom to $L = 12$, 16.97, 18.97, 20.78, and 24. The dashed line is the $4\epsilon^{-1}T = 1$ curve.

In order to locate the phase transition point we performed a fit based on the finite size scaling formula (40). The procedure is as follows: One picks values of the inverse dielectric function, $\widehat{\epsilon^{-1}}\left(\frac{2\pi}{L}\right)$, calculated for different values of T and L. For each value of the temperature one tries to fit the dependence of $\widehat{\epsilon^{-1}}\left(\frac{2\pi}{L}\right)$ on L to the finite-size scaling formula (40) by minimizing the χ^2-error function

$$\chi^2(T) = \sum_i \left\{ \epsilon^{-1}(T, L_i) - 4T \left[1 + \frac{1}{2\log(L_i/L_0)} \right] \right\}^2 \tag{45}$$

with respect to the parameter L_0. The summation runs over the different system sizes, L_i.

The assumption is that there exists a single temperature T_c for which

$$\lim_{\forall i, L_i \to \infty} \chi^2(T_c) = 0. \tag{46}$$

The numerically estimated value of T_c is therefore the one that minimizes the error function $\chi^2(T)$. In order for this estimate to be meaningful, it has to be independent of the set of system sizes used for this minimization. To verify that this is indeed the case, we repeated this procedure for various sets of system sizes, and checked that the minimum does not vary much.

The dependence of the χ^2-error on the temperature is shown in Figure 7. The three curves were obtained with fitting procedures including sets of 3, 4, and 5 different system sizes. All three curves have a minimum in which the χ^2-error is small, namely of the order of the sampling error. This minimum point constitutes the numerical estimation for the phase transition point. Thus for $n = 0.0277$ we evaluate the phase transition point to be $T_c = 0.0805$.

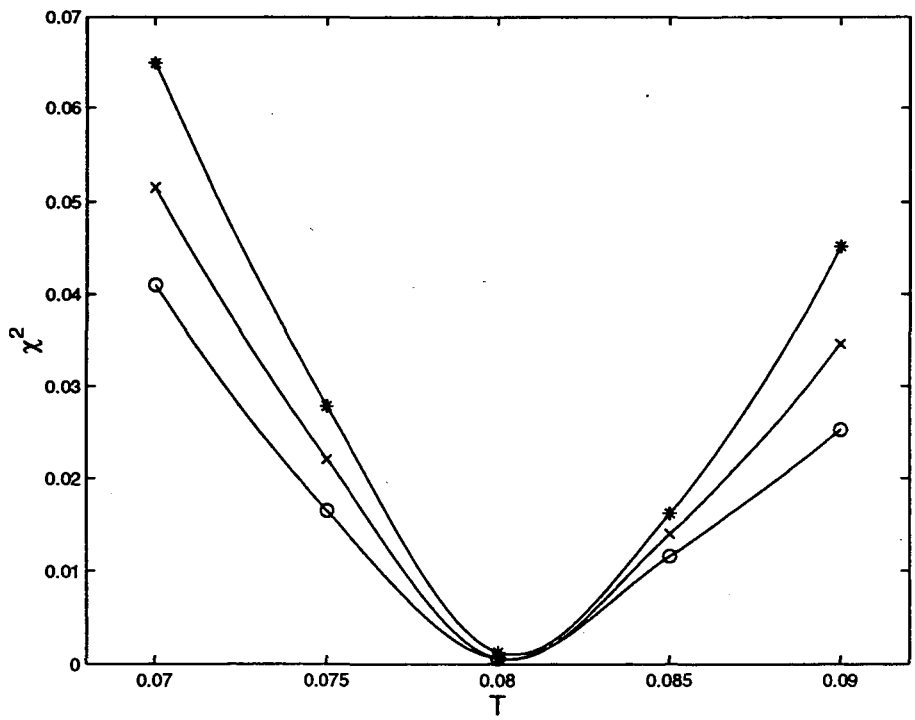

Figure 7: The fitting procedure for the canonical ensemble: χ^2-error of the fit versus temperature for $L = [12, 16.97, 18.97]$ (stars), $L = [12, 16.97, 18.97, 20.78]$ (crosses), and $L = [12, 16.97, 18.97, 20.78, 24]$ (open dots). These curves have a minimum around $T \simeq 0.0805$. The fitted value of L_0 is 1.43 ± 0.01.

A similar set of calculations was repeated for the grand-canonical ensemble. In Figure 8 we plot $\widehat{\epsilon^{-1}}\left(\frac{2\pi}{L}\right)$ versus the temperature. Unlike in Figure 6 the dielectric function is not monotonically decreasing as the size of the system increases. The five curves approximately intersect at the point $T \simeq 0.085$. Such an intersection point was interpreted in [22] as the location of the phase transition point. It is however unclear whether more curves are going to intersect the same point at larger system size. In fact, Figure 6 indicates that curve intersection cannot be generally used as a criterion to locate the phase transition point.

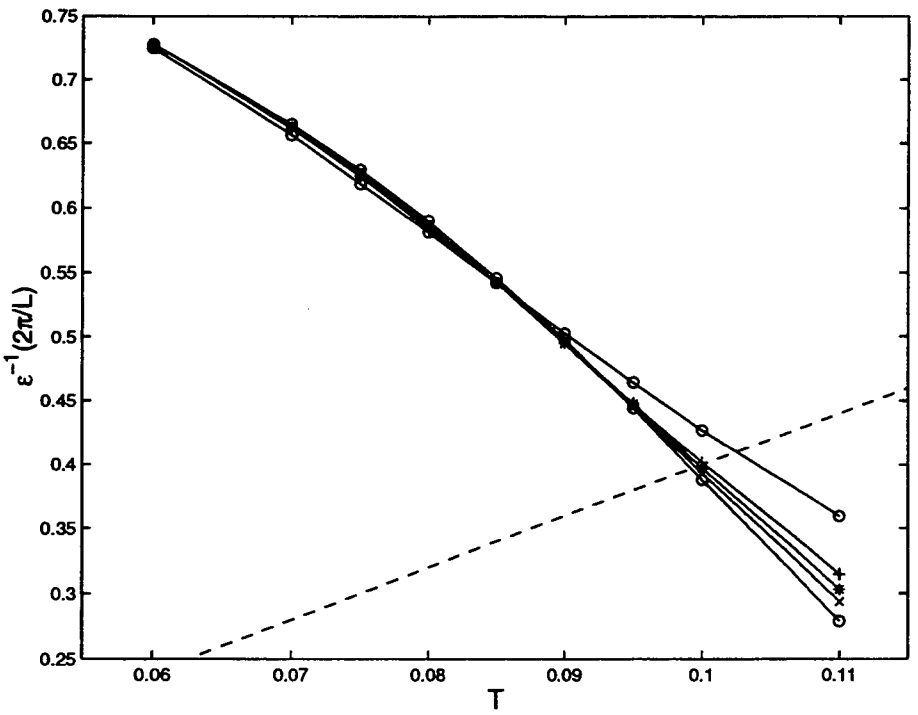

Figure 8: Grand-canonical ensemble: the inverse dielectric function for the smallest nonzero wavevector as function of temperature. The fugacity is $\bar{z} = 0.006$. The five curves correspond to $L = 12$, 16.97, 18.97, 20.78, and 24. The dashed line is the $4\epsilon^{-1}T = 1$ curve.

The corresponding χ^2-error is plotted versus the temperature in Figure 9. The error function vanishes within the expected accuracy at $T_c \simeq 0.096 \pm 0.001$, which indeed does not coincide with the point where the five curves intersect.

In the grand-canonical ensemble we can also calculate the average density of dipoles, $\langle n \rangle$; it is plotted in Figure 10 as function of temperature for the five different system sizes. An intriguing result is that the density is a *decreasing* function of the size of the system. This cannot be reconciled with the finite-size relation (42) as $n(r)$ is by the definition of the KT model a monotonically increasing function of r. We have not found an adequate explanation

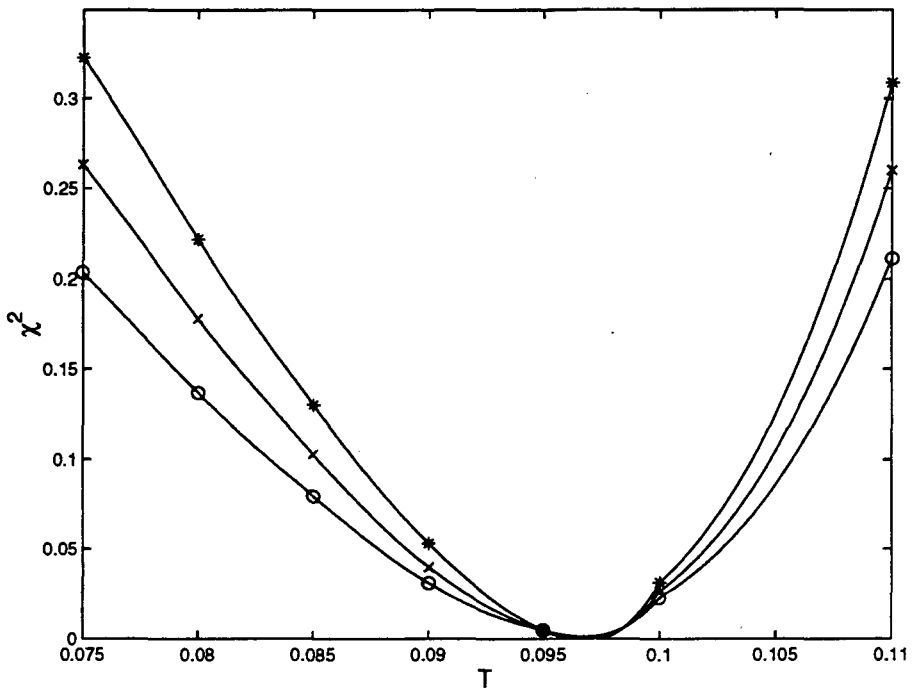

Figure 9: The fitting procedure for the data of Figure 8: χ^2-error of the fit versus temperature for $L = [12, 16.97, 18.97]$ (stars), $L = [12, 16.97, 18.97, 20.78]$ (crosses), and $L = [12, 16.97, 18.97, 20.78, 24]$ (open dots). These curves attain a minimum around $T \simeq 0.096$.

for this observation.

Once we have a well-defined procedure to calculate the phase transition point, the phase transition line, $T_c(\bar{z})$, can be traced. This is shown in Figure 2 where the values calculated from the Monte-Carlo simulations are represented by open dots, whereas the solid line is the theoretical prediction obtained by a numerical integration of the RG equations (25). The agreement between the two is remarkable.

For the average density of dipoles, $\langle n \rangle$, a similar comparison between the simulations and the RG equations is problematic; in the absence of an appropriate finite-size scaling formula we are unable to estimate accurately the $L \to \infty$ limit of the dipole density. In Figure 11 we plot $\langle n \rangle$, as function of the fugacity, $\bar{z}$, at the phase transition line. The solid line is again the theoretical expectation; the open dots represent the simulation results for the largest system ($L = 24$), and because $\langle n \rangle$ is apparently a decreasing function of L, they constitute only an upper bound.

The inability to estimate accurately the density of dipoles in the thermodynamical limit make it difficult to compare the numerical results in the canonical and the grand-canonical

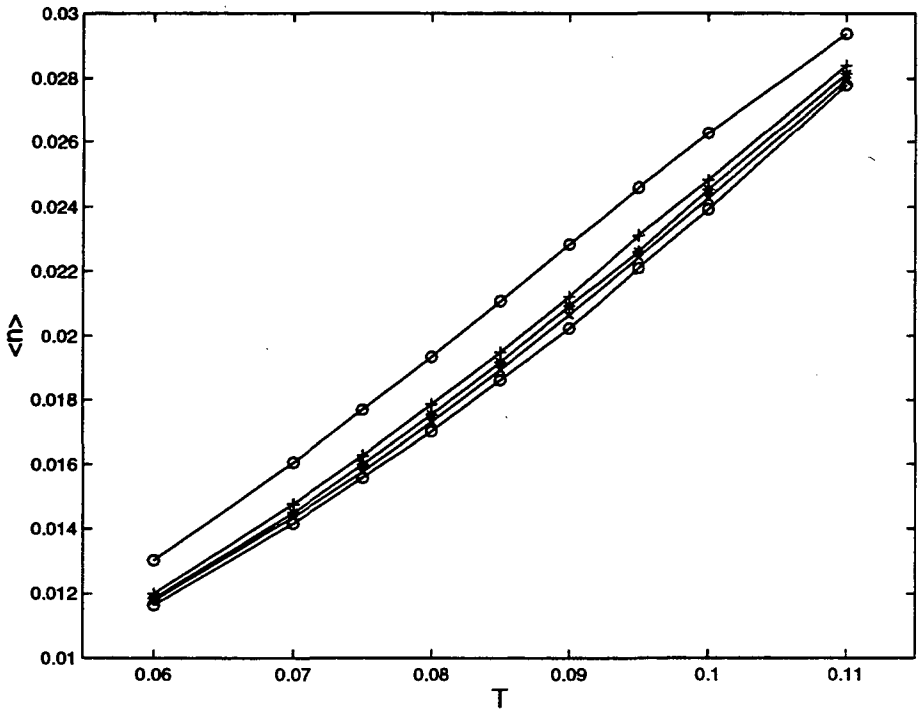

Figure 10: Grand-canonical ensemble: the average density of dipoles as function of temperature. The fugacity is $\bar{z} = 0.006$. The five curves correspond from top to bottom to $L = 12$, 16.97, 18.97, 20.78, and 24.

ensembles. We can only perform a rough test of consistency based on our upper bound for the dipole density in the grand-canonical ensemble. For a dipole density of $n = 0.0277$, an interpolation based on the data points shown in Figure 11 gives a corresponding fugacity of $\bar{z} \simeq 0.0082$. From Figure 2 the critical temperature for this value of the fugacity is $T_c \simeq 0.085$, i.e., about 5% off the calculated transition point for the canonical ensemble sampling.

We have treated the parameter L_0 as a free parameter selected by the procedure in which the calculated values of $\widehat{\epsilon^{-1}}\left(\frac{2\pi}{L}\right)$ were fitted to the finite size scaling formula (40). Given a model, L_0 is not a free parameter, but results from the renormalization equations. We now compare the value of L_0 obtained from the fitting procedure to the expectation value from the KT model.

For $\bar{z} = 0.006$ as analysis of the renormalization equations gives $\frac{2}{4-K} \sim \ell + 0.695$, which means that $L_0 = e^{-\ell_0} = 0.499$. In Figure 12 we plot the values of L_0 as calculated from the fitting procedure as function of temperature. For this value of the fugacity the critical temperature was evaluated as $T_c = 0.096 \pm 0.001$, which implies that $0.3 < L_0 < 1.0$. Within

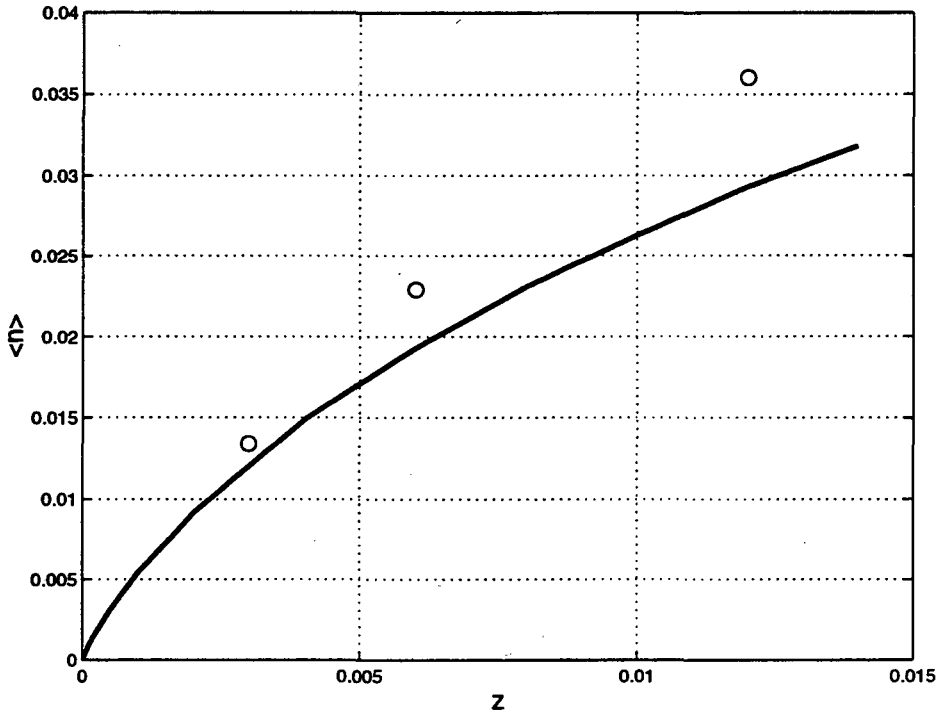

Figure 11: The density of pairs, $\langle n \rangle$, as function of the fugacity, $\bar{z}$, for the critical temperature, $T_c(\bar{z})$. The solid line is the result of the RG equations; the open dots are the Monte-Carlo simulation results for $L = 24$.

the given accuracy of our procedure the numerical estimate of L_0 is not accurate enough to allow a sharp test of the KT model. The most we can claim is that the numerical estimate of L_0 agrees with the theoretical expectation within a factor of two.

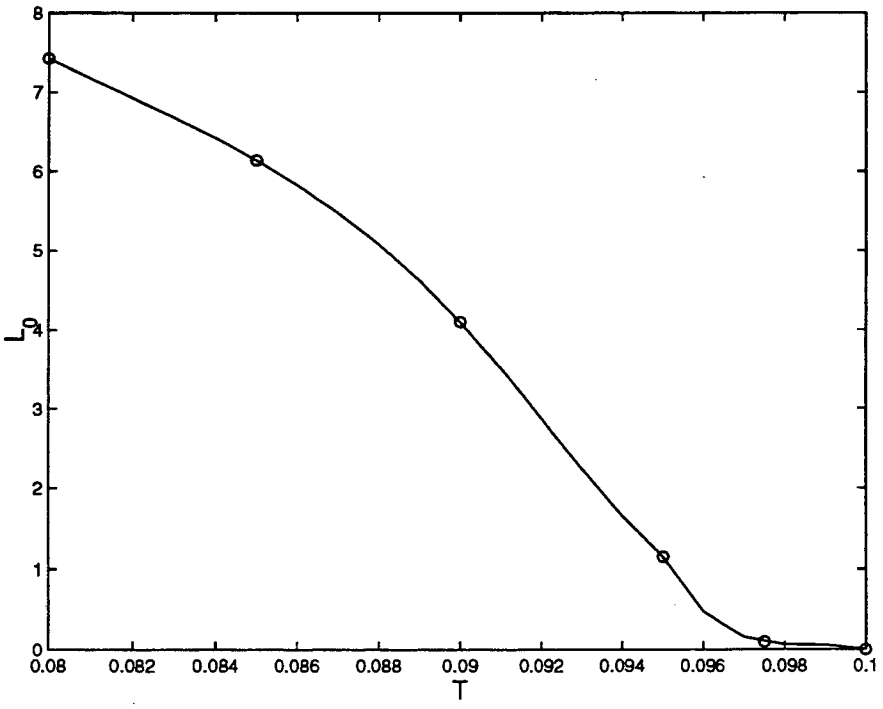

Figure 12: The fitting parameter L_0 as function of temperature for $\bar{z} = 0.006$.

7 Discussion

The salient conclusion from our calculations is that the KT renormalization flow predicts correctly the phase transition line in a KT transition, and thus that the conclusions from the one-sided polarization assumption are correct, at least for the infinite-size limit of a system of finite size. The calculations use in an essential way the form of finite-size scaling derived from the KT equations, but do not depend on the precise values of the coefficients in that scaling. The calculations also utilize the Nelson universal-jump assumption, for which an independent check would have been desirable. The least one can say is that the KT theory is self-consistent. Among the numerical questions that remain inadequately analyzed are: (i) The surprising behavior of the number density n as a function of the system size; (ii) the inconsistent behavior of the intersections of the finite-size transition curves, which should have offered a reliable alternative to the localization of the transition points via the universal jump assumption, and (iii) the failure of the "self-consistent" boundary conditions to provide an alternative path to the reduction of finite-size effects. We can offer no method for checking the alternate models of [14].

In view of these results, we shall feel fully justified in using the KT theory as a starting point for the analysis of dynamical effects in the neighborhood of the critical line in Coulomb and vortex systems. These calculations will be presented in a subsequent publication.

Acknowledgments

We would like to thank Profs. O. Hald, O. Knio and H. Weber for helpful discussions and comments. We thank Profs. J. Lidmar and M. Wallin for explanations, and for making their computational code available. This work was supported by the Applied Mathematical Sciences Subprogram of the Office of Energy Research, Department of Energy, under Contract Number DE-AC03-76SF-00098.

References

[1] J. Kosterlitz and D. Thouless, *J. Phys. C: Solid State Phys.* **6**, 1181 (1973).

[2] D. Amit, Y. Goldschmidt, and G. Grinstein, *J. Phys. A: Math. Gen.* **13**, 585 (1980).

[3] P. Minnhagen, *Phys. Rev. B* **32**, 3088 (1985).

[4] P. MINNHAGEN and M. WALLIN, *Phys. Rev. B* **36**, 5620 (1987).

[5] T. SAITO and H. MÜLLER-KRUMBHAAR, *Phys. Rev. B* **23**, 308 (1981).

[6] J. TOBOCHNIK and G. CHESTER, *Phys. Rev. B* **20**, 3761 (1979).

[7] H. WEBER and P. MINNHAGEN, *Phys. Rev. B* **37**, 5986 (1988).

[8] P. OLSSON, *Phys. Rev. B* **46**, 14598 (1992).

[9] P. OLSSON, *Phys. Rev. Lett.* **73**, 3339 (1994).

[10] P. OLSSON, *Phys. Rev. B* **52**, 4511 (1995).

[11] P. OLSSON, *Phys. Rev. B* **52**, 4526 (1995).

[12] P. GUPTA and S. TEITEL, Phase diagram of the two dimensional lattice Coulomb gas, preprint cond-mat/9609031, 1996.

[13] J. LIDMAR and M. WALLIN, *Phys. Rev. B* **55**, 522 (1997).

[14] A. CHORIN and O. HALD, *Physica D* **99**, 442 (1997).

[15] A. YOUNG, *Phys. C : Solid State Phys.* **11**, L453 (1978).

[16] A. ALASTUEY and F. CORNU, *J. Stat. Phys.* **66**, 165 (1992).

[17] G. BARENBLATT and A. CHORIN, *Appl. Mech. Rev.* **50**, 413 (1997).

[18] P. MINNHAGEN, *Rev. Mod. Phys.* **59**, 1001 (1987).

[19] M. ABRAMOWITZ and I. STEGUN, *Handbook of mathematical functions with formulas, graphs, and mathematical tables*, Dover, New York, 1971.

[20] D. NELSON and J. KOSTERLITZ, *Phys. Rev. Lett.* **39**, 1201 (1977).

[21] D. AMIT, *Field theory, the renormalization group, and critical phenomena*, World Scientific, Singapore, 1984.

[22] J.-R. LEE and S. TEITEL, *Phys. Rev. Lett.* **64**, 1483 (1990).

[23] H. WEBER, *Monte Carlo simulations in connection with superconducting films and XY-model*, PhD thesis, University of Umeå, Sweden, 1988.

[24] J.-R. LEE and S. TEITEL, *Phys. Rev. B* **46**, 3247 (1992).

[25] K. BINDER, *Theory and "technical" aspects of Monte-Carlo simulations*, pp. 1–46, Springer-Verlag, Berlin, 1979.

[26] A. CHORIN, *Commun. Math. Phys.* **99**, 501 (1985).

Ernest Orlando Lawrence Berkeley National Laboratory
One Cyclotron Road | Berkeley, California 94720

Prepared for the U.S. Department of Energy under Contract No. DE-AC03-76SF00098